Fibers and Polymers 2020, Vol.21, No.7, 1466-1474
DOI 10.1007/s12221-020-9904-x

ISSN 1229-9197 (print version)
ISSN 1875-0052 (electronic version)

Nanofibrous Membranes with High Air Permeability and Fluffy Structure based on Low Temperature Electrospinning Technology

Siying Lin[1], Xiang Huang[1], Zhenxiang Bu[1], Zhihong Lin[1], Peiqin Xie[1], Xiaolong Lin[1], Lingyun Wang[1]*, and Wenlong Lv[2]*

[1]*Department of Mechanical and Electrical Engineering, Xiamen University, Xiamen, Fujian 361005, China*
[2]*Pen-Tung Sah Institute of Micro-Nano Science and Technology, Xiamen University, Xiamen, Fujian 361005, China*
(Received August 27, 2019; Revised November 1, 2019; Accepted November 9, 2019)

Abstract: Due to its small diameter and high density, electrospun nanofiber membranes have high resistance which obstacles their application. In this paper, we proposed a new electrospinning method based on low-temperature, which can affect the deposition process of electrospinning by utilizing the freezing process of steam in the receiving plate. The filling and supporting of ice could enlarge the pores of membranes and intervals among fibers, which caused the high porosity (92 %), rough surface, fluffy structure and low pressure drop (123 Pa) of polyvinylidene fluoride (PVDF) nanofibrous membranes. The results suggested that the electrospinning method is a promising way to prepare nanofibrous membranes with high air permeability and fluffy structure for air filtration.

Keywords: Electrospinning, Nanofibrous membranes, Air permeability, Pressure drop, Porosity

Introduction

In recent year, the deterioration of air quality and constant hazy weather seriously threaten the human life and health seriously [1]. Particularly, fine particles smaller than 2.5μm in diameter are considered to be the main cause of health effects in the respiratory tract and extrapulmonary organs [2]. Without doubt, there is a great need to develop better filter materials and separation technologies to prevent harmful fine particles from getting into the environment and the human body. Traditional fibers, including glass fibers, melt-blown fibers, and spun-bonded fibers, cannot capture fine particles due to their small fiber diameter [3]. The nanofibrous membranes based on electrospinning technology, referring to fibers with diameter less than 500 nm, and it is a promising medium. It has higher filtration efficiency and better performance than conventional fibers. It has received considerable attention in filtration applications [4].

The fibrous membrane produced by electrospinning has high porosity, an interconnected porous structure, and significant special surface area [5]. For all of these reasons, electrospinning technology has potential applications in air purification. Venkataraman used electrospinning process to produce flexible polyurethane and polyvinylidene fluoride nanofibers embedded with silica aerogel [6,7]. Na Wang developed electrospun PAN nanofibers with a diameter of 300-500 nm, which can filter 99.989 % of sodium chloride particles [8]. Other scholars also showed that the filtration efficiency of nanofibrous membranes can reach over 99 % [9-11]. And the group of professor Huang did a lot works to improve the air filtration [12,13], including the preparation of ecofriendly cross-linked blend PVA/KGM electrospun nanofiber membranes loaded with ZnO nanoparticles which the filtration efficiency was higher than 99.99 % [13]. Moreover, Ran Wang and Xiaoliang Wang have realized the filtration of bacteria, virus and protein through electrospun fibrous membranes [14,15]. All these researches have proved that electrospun nanofiber membrane has extremely high filtration efficiency.

The smaller fiber diameter of nanofibrous membrane caused the increasing of fiber numbers in per unit area and fiber layers in the thickness direction, which result in the decrease of pore diameter to hit the mark of increasing interception [16,17]. However, the improvement of filtration efficiency may lead to some consequences, including the poor air permeability, increasing packaging density and air resistance. The thicker of filtration membranes are, the longer of flow path will be, and the more particles will be trapped and blocked by fiber [18]. However, the air resistance will also rise at the same time. The filtration resistance of ordinary electrospun nanofibrous membranes can reach up to 1600 Pa [19], so that we can only resist the high resistance phenomenon which caused from the fine fiber diameter by decreasing the thickness of filtering membranes in the application [20]. What should be mentioned is that the decreased thickness can not only reduce the filtration efficiency and mechanical strength of membranes, but also shorten the dust absorption and service life of nanofibrous membranes. It can seriously hinder the application and development of electrospun nanofibrous membranes. Therefore, how to reduce air resistance of nanofibrous membranes while maintaining the filtration efficiency is an urgent problem to be solved.

To solve this contradiction, some research teams have prepared high-efficiency and low filtration resistance

*Corresponding author: wangly@xmu.edu.cn
*Corresponding author: lwl1980@xmu.edu.cn

nanofibrous membranes by using composite membranes, such as electrospun membranes with different density [21], nano/micron-multilayer composite materials [22,23], electrospinning and fabric composites [24,25]. These methods make filtration efficiency reach up to 99 %, filter resistance reached 300-500 Pa. While other scholars add some inorganic particles and pore-foaming agents, such as titanium dioxide particles [26,27], silicon dioxide nanoparticles [28, 29], silver and NaCl [30,31] to increase the porosity of nanofibrous membranes and decrease the air resistance. Although these methods have made some achievements, they cannot be applied into practical for they need complicated technology and adhesions in composition or affect the mechanical properties of products when adding some particles. Li Bao found that filter membranes remained diameter at around 100 nm and stacked evenly, they can achieve low dropout and high efficiency through slip phenomenon, but their service life should be prolonged [32, 33]. In addition, some scholars have taken the methods, such as taking electrospinning with mixed spinning solution and changing the structure of receiving device, to change the filtering quality of nanofibrous membranes, pore structures and stacking density [34,35]. Marc Simonet investigated a method to substantially increase the degree of porosity in the third dimension by using ice crystals as removable void templates [36]. Unfortunately, the results do not work so well. There are few simple and effective ways to decrease the filter resistance of nanofibrous membranes at present. Therefore this paper aims to study a method for preparing nanofibrous membranes with low resistance and high filtration efficiency.

In this paper, we describe a method that can affect the deposition process of electrospining, by using the freeze of steam in the receiving plate, and the device diagram is shown in Figure 1(a), which includes a power supply, a syringe pump, and a refrigerating board. Traditional electrospun nanofibers (Figure 1(d)) were proceeding under the room temperature (25 ^{o}C), while we deposited nanofibers membranes under low-temperature, which are shown in Figure 1(b) and (c). From the diagrams, we can see that the steam can achieve liquefaction and solidification on the refrigeration receiving plate. And the ice acted as a scaffold to support the depositional fibers following the frozen and electrospinning continually, which can increase the distance of the layers of fibers, and dilate the nanofiber scaffold and pores can be seen in Figure 1(e).

The asymmetrical solidification and ablation of ice could cause the self-supporting of fibers. The ablation of ice inside membranes enlarged the porosity and connectedness, but rougher at the same time. Therefore, the PVDF nanofibrous membranes have high fluffy structure and air permeability. The focus of this paper is to investigate the effects of temperature on the thickness, porosity and pressure drop of nanofibrous membranes. A new method for preparing nanofiber membrane with high filtration efficiency and low filtration resistance was further explored.

Experimental

Materials

In the electrospinning, the spinning solution should be insoluble in water due to the presence of water. Polyvinylidene fluoride (PVDF) is used as low-temperature spinning raw material, which has the characteristics of high mechanical

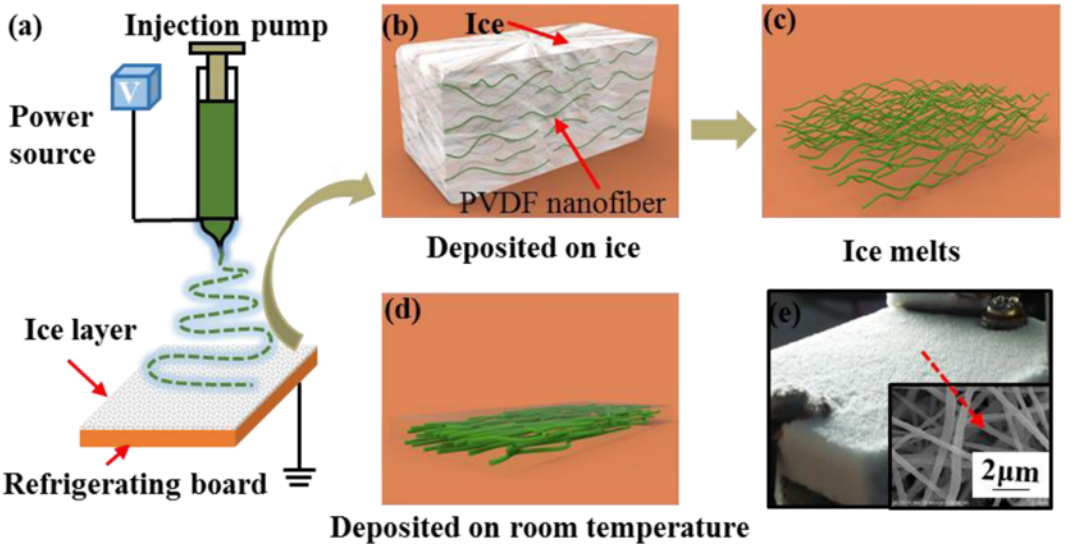

Figure 1. Diagram of low-temperature electrospun device and nanofibers membrane at different temperatures; (a) the diagram of low-temperature electrospun device, (b), (c) the depositing process of PVDF nanofibrous membranes with low-temperature technology, (d) the PVDF nanofibrous membranes of deposition on room temperature, and (e) representation of the PVDF nanofibrous membranes on ice layer.

strength, heat resistance, anti-corrosion, non-toxic and insoluble in water. PVDF (MW=~534000) was purchased from Sigma-Aldrich Co., Ltd., USA. N-Methyl pyrrolidone (NMP) and acetone was supplied by Sinopharm Chemical Reagent Co., Ltd. China. All chemicals were of analytical grade and were used without further purification.

Preparation of Nanofibrous Membranes

The preparation procedures of nanofibrous membranes are as follows. PVDF solution at concentrations 16 % were prepared by dissolving PVDF in a binary solvent system of N-Methyl pyrrolidone (NMP) and acetone at a fixed ratio of 5:5, then stirring for 24 h. The PVDF solution was loaded into a 2.5 m*l* syringe with a metal needle (27G), and then mounted in a programmable syringe pump (D-301525 Harvard Apparatus Co., USA) at a feed rate of 200-400 μ*l*/h. A high voltage of 6-8 kV was applied to the needle tip through a high-voltage supply (DW-P503-1ACDF, Tianjing Dongwen High Voltage Co., China) to produce a continuous jet. The ambient temperature and humidity were 25 °C and 55 %, respectively. The PVDF nanofibrous membranes were deposited on the frore receiving plate acquired by refrigerating board at a 10 cm tip-to-collector distance. The receiving plate consists of semiconductor refrigeration piece, water cooling system and thermoregulator, etc. Simultaneously, the receiving device was installed in XY mobile platform to obtain uniform nanofiber membrane. The temperature range of substrate controls between -11 °C and 25 °C by the thermoregulator. The deposition time of nanofibrous was controled within 6 h. The PVDF nanofibrous membranes were prepared by natural air-dry after electrospinning under low temperature.

Characterizations of PVDF Nanofibrous Membranes

The surface and cross-sectional morphology of membranes were observed by using a field emission scanning electron microscope (FE-SEM) (J-60, Hitachi Ltd., Japan). All specimens were gold-coated for 45 s (E1045, Hitachi ion, sputter, Japan). Cross-sectioned views were obtained from the fracturing of the membranes after the liquid nitrogen freezing treatment. The diameter and distributions of each fibrous mat were measured by an image analyzer (Adobe Photoshop CS2). The deposition of nanofibrous at different temperature of collection plate was recorded with a CCD camera. The thickness of PVDF nanofibrous membranes was measured by a laser displacement sensor.

Porosity is one of the important indexes for measure the fluidity of nanofibrous membranes. It defines the ratio of the pore volume to the membrane volume. The porosity of the nanofibrous membranes was measured by the n-butanol method, which was calculated by the following equation (1):

$$\varepsilon = \frac{(m_1 - m_0)/\rho_1}{(m_1 - m_0)/\rho_1 + m_0/\rho_2} \quad (1)$$

where ε is the porosity of the PVDF fibrous membranes, m_0 is the mass of the dry membrane, and m_1 is the mass of membrane after immersion in n-butanol, ρ_1 and ρ_2 is the density of n-butanol and PVDF fibers respectively.

The air permeability of fibrous membranes mainly reflects in pressure loss, and also means the filter resistance when filtering the fluid. Pressure drop could reflect the breathability of membranes perfectly. This paper adopts the pressure drop test device shown in Figure 2(a). Gases flow the sample filter under the action of a vacuum pump, and the modular pressure controller tests the pressure of both sides

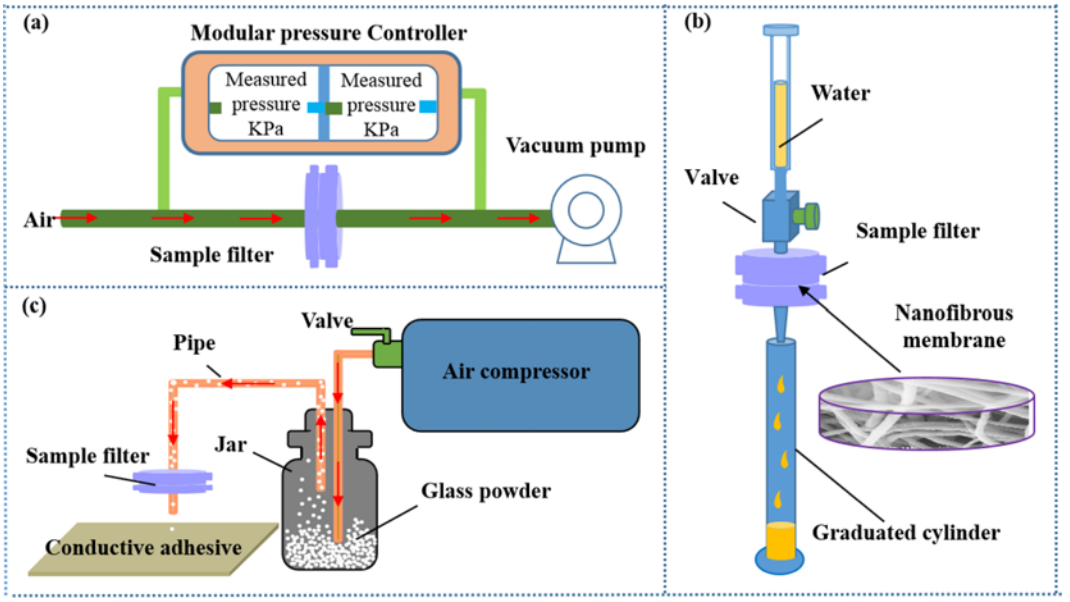

Figure 2. Devices of sample test; (a) pressure drop test device, (b) the device of liquid filtration, and (c) the device of air filter.

of filter, then the pressure drop of gas can be obtained. Just as Figure 2(b) shows, the connectedness of membranes and fluid resistance can be seen by measuring the time of liquid flowing through the membranes per unit volume. The hydrophobicity of PVDF membranes should be soaked in the straight alcohol for 4 hours to get it wet before the experiment.

In order to test the filtration performance of PVDF nanofiber membranes prepared by low-temperature electrospinning, a filter device as shown in Figure 2(c) was

Table 1. Electrospinning processing conditions for PVDF

Concentration (%)	Voltage (kV)	Flow rate (μl/h)	Receiving distance (cm)
16	6	200	10
16	6	400	10
16	7	200	10
16	7	400	10
16	8	200	10
16	8	400	10

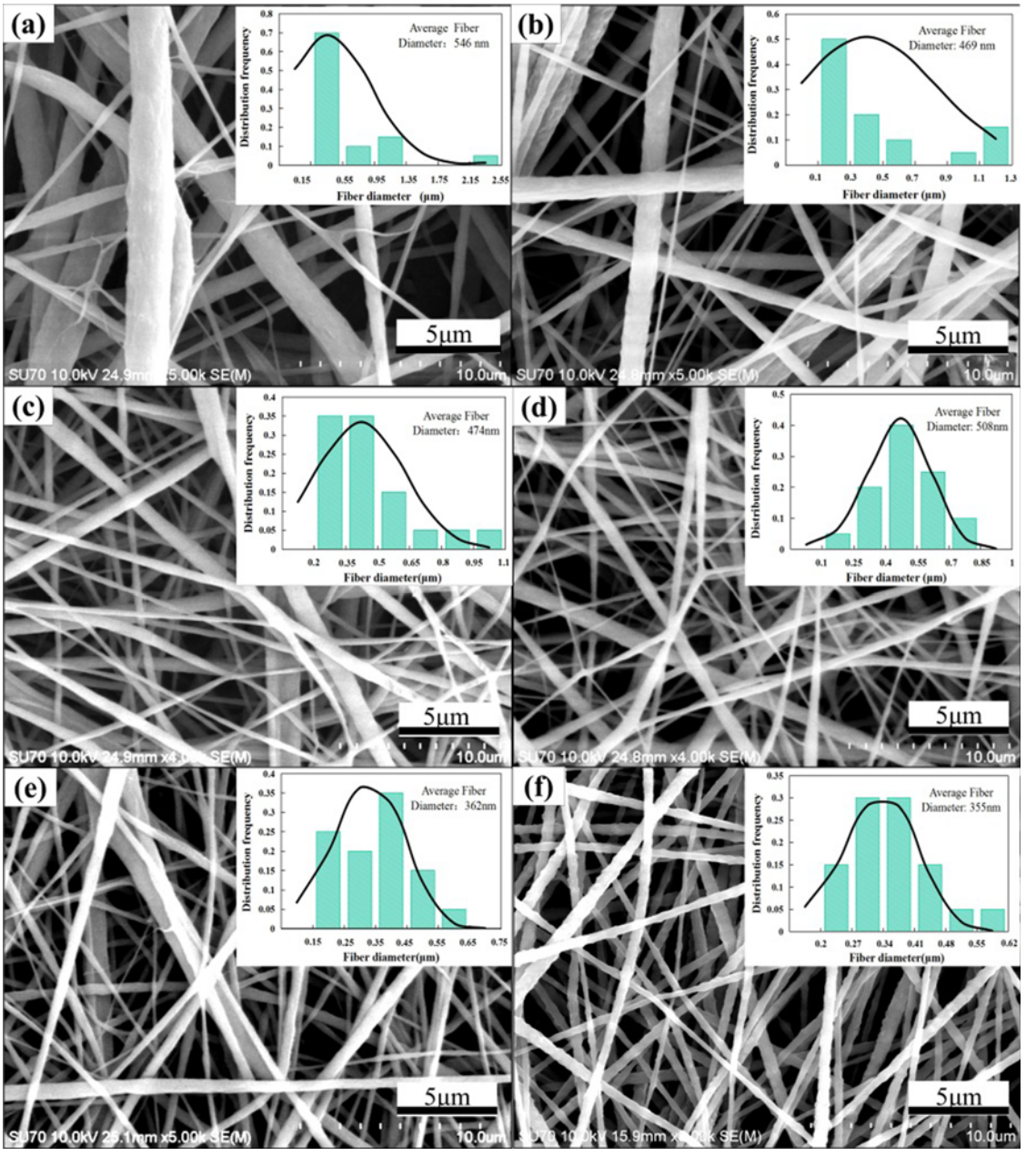

Figure 3. Distribution statistics of fiber diameter and SEM images of PVDF nanofiber membranes under different parameters; (a) 6 kV 200 μl/h, (b) 6 kV 400 μl/h, (c) 7 kV 200 μl/h, (d) 7 kV 400 μl/h, (e) 8 kV 200 μl/h, and (f) 8 kV 400 μl/h.

designed. The way in which air is filtered by fiber membrane is mainly to remove the micro-nano scale particles. Glass powder is used to simulate the particles in the air to test the filtrating effect of filter membrane. The airflow generated by the air compressor blows the glass powder from the jar into the sample filter, passed through the filter membrane, and finally collected at the bottom of the pipe through the conductive adhesive. The collected particles were observed under SEM for statistical analysis.

Results and Discussion

Probing of Stable Electrospinning Conditions

Technological parameters of electrospinning process mainly include voltage, flow rate and receiving distance. Voltage and flow rate mainly influence the uniformity, efficiency and size of fiber diameter, while the receiving distance affects the production of bead. To get the steady electrospinning conditions, the parameters of configured PVDF solution were set as Table 1.

Figure 3 shows the normal distribution statistics of fiber diameter and SEM images of PVDF nanofiber membranes. According to the figure, we can conclude that the voltage and flow rate remain small, the fiber diameter distribute unevenly and the morphology will be more different. For example, when the parameter is set as 6 kV, 200 μl/h, then the coarse diameter surpasses 2 μm and the finest remains 200 nm (Figure 3(a)). As bias voltage and flow rate increasing, average diameter of fiber is gradually decreasing, and its distribution is changed from dispersion to even. When bias voltage is 8 kV and flow rate is 400 μl/h (Figure 3(f)), fiber is the most even and its average diameter is about 355 nm. Therefore, the parameters are selected as the conditions for electrospinning.

Morphology and Fluffy Structure of the PVDF Membranes

PVDF nanofibrous accumulate on the ice layer of collector, and the thickness of membrane is influenced by the rate of snowing. As the temperature of the receiving plate is continuously lowered, the formation speed of the snowflake is accelerated and the ice accumulation among the fibers is increased, which lead to an accelerated increase in the thickness of the nanofiber film. From the process of electrospun, we can get that the temperature remains at -9 °C, the thickness grows fastest, but when the temperature is above 0 °C, the thickness would be similar under various temperatures due to the vapour would only liquefaction, without solidification.

Figure 4 shows the surface structure of both traditional room-temperature and low-temperature electrospun PVDF nanofibrous membranes. The surface of traditional membranes (Figure 4(a)) was smoother and denser, and fibers superimposed more tightly, while the surface of the low-temperature pattern (Figure 4(b)) was rougher with some

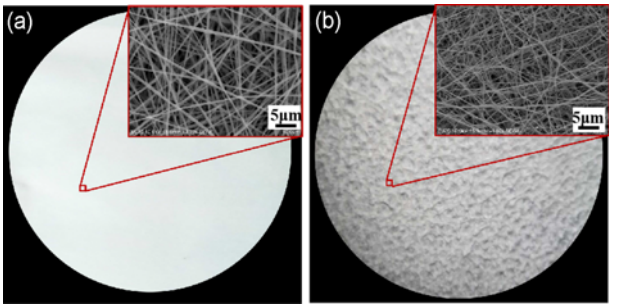

Figure 4. PVDF nanofibrous membranes of different temperature eletrospun; (a) the traditional room-temperature and (b) the low-temperature electrospun.

embossment, and the fibers superimposed more loosely. The collapsed of three-dimensional structures caused by the melted of ice layer could lead to no stable support among fibers, and forming the membranes with littery and rough surface.

The surface and cross-sectional SEM images of PVDF nanofiber membranes at different electrospun temperatures are shown in Figure 5. As the temperature decreases, the gap becomes wider, the structure becomes looser and the amount of fibers in per unit area of surface and the vertical direction becomes less. In the cross-sectional images (Figure 5(b)), the space among layers will be larger following the decreasing of temperature. There are two main reasons for the expansion of the membrane structure. One is that the filling and supporting of ice can enlarge the pores of membranes and intervals among fibers. The other is that the uneven deposition and collapse of fibers in vertical direction caused self-supporting so as to improving the fluffy of membranes and connectedness of pores.

The thickness of PVDF membranes under various temperature changes with electrospun time reflected in Figure 6(a). From the figure, we can get that the thickness of PVDF nanofibrous membranes was thicker with the decrease of temperature during the same electrospun time. It indicates that the expansion scaffold formed by the filling of ice in the nanofiber membrane still exists after melting, and the intumescent effect will be more obvious with lower temperature. Simultaneously, the homogeneity of thickness will be worse with the lower temperature. There are two main reasons for the unhomogeneity, one is the fast and uneven freezing rate of ice on the substrate surface, the other is the flowing aggravation of ice water after melting.

Figure 6 (b) presents the porosity and packaging density of PVDF membranes under the various electrospun temperatures. Among these, the calculative porosity (2) and packaging density (3) can be calculated by following equations:

$$\alpha = \frac{Q}{L\rho_2} \tag{2}$$

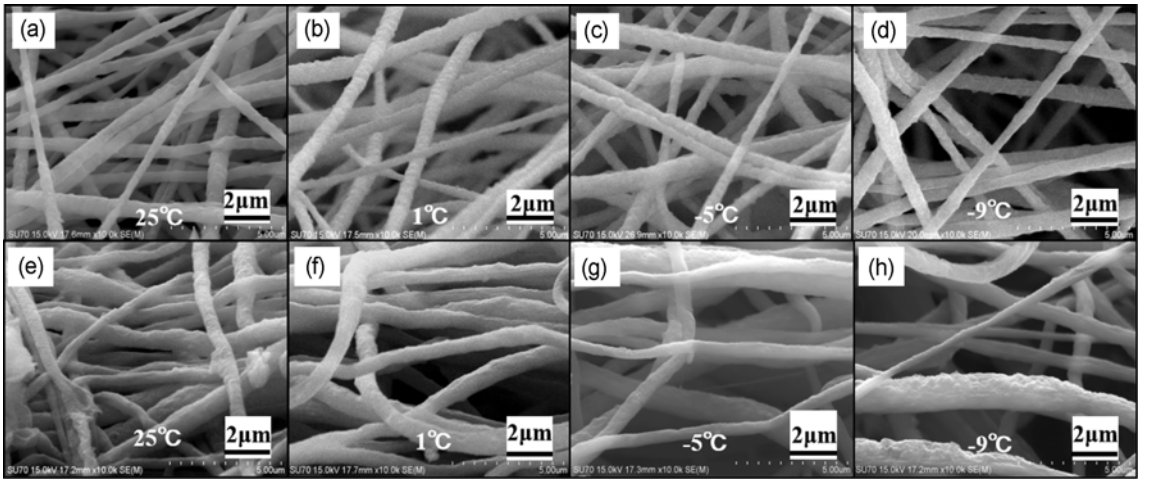

Figure 5. Surface (a-d) and cross-sectional (e-h) SEM images of PVDF nanofiber membranes with different electrospun temperatures.

$$\varepsilon_C = 1 - \alpha \tag{3}$$

where α is the packaging density of PVDF nanofibrous membranes, Q is the mass thickness, L means geometry thickness, and ε_c is the calculation porosity. It is obvious that the calculation porosity is almost consistent with experimental results. The porosity of traditional and low-temperature technology ranges from 70 % to 75 %, 80 % to 92 % respectively. The porosity reaches over 90 % when the temperature is lower than -5 °C, which is 10-20 % higher than traditional technology. Obviously, the change of packaging density is consistent with the change of porosity.

The above results indicate that the PVDF nanofibrous membranes prepared by low-temperature electrospinning technology have the characteristics of higher porosity, looser and fluffier structure than that prepared by normal-temperature.

Permeability of the PVDF Membranes

It can be seen from Figure 6(c), the pressure drop of the electrospun PVDF membranes that electrospinning at the same time and at different temperature varies linearly with the inlet pressure. It can reflect that the pressure drop of nanofibrous membranes based on normal-temperature elelctrospinning technology can ranges from 600 Pa to 1700 Pa. However, the pressure drop of low-temperature electrospinning technology is obviously lower than that of normal-temperature, and the minimum pressure drop (100-500 Pa) is presented at the temperature of -5 °C. Since there is no ice, the pressure drop at 3 °C is close to room temperature. These phenomena indicate that the PVDF nanofibrous membranes based on low-temperature electrospinning technology have better air permeability than that of normal-temperature. Figure 6(d) shows the thickness and pressure drop of PVDF membranes based on the same time of electrospinning at different temperatures. Interestingly, the pressure drop of -5 °C is lower than that of -7 °C and -9 °C. One possible explanation is that the thickness of the PVDF membranes at -5 °C. Likewise, the pressure drop between -7 °C and the -9 °C is close due to the thickness effect. Figure 6(e) shows the removal efficiency of the membranes after multiple filtration cycles. The filtration efficiency of the membrane (16 %wt, -5 °C) was tested 20 cycles, it also can be seen that the filtration efficiency maintains more than 95 %.

To verify the air permeability and connectedness of membranes with the same thickness at different electrospun temperature, some PVDF nanofibrous membranes were prepared with similar thickness according to the rules shown in Figure 6(a). The results are shown in Table 2. The pressure drop of PVDF nanofibrous membranes can decrease to 123 Pa at -7 °C with a thickness of 83 μm, far below the 620 Pa at normal temperature with 90.6 μm. It can be concluded that the pressure drop of membranes decrease obviously with lower temperature when their have similar thickness. From the Figure 7 we can see that, the lower the temperature is, the faster the liquid flows through the membrane, which means that the membrane connectivity is better. That is because the fluid flows out of membranes when ice melting, passing-through the pores. Among then, the liquid flows the fastest with only 14 seconds at -7 °C, while at 3 °C and 25 °C, the liquid velocity is close due to the absence of icing.

All above results show that the air permeability and pore connectedness of electrospun nanofibrous membranes at low-temperature are better than those of the electrospun membranes at room temperature. It is proved that the comprehensive performance of PVDF membranes achieves the best when the temperature remains at -5 °C at the same amount of electrospun time. We also explored the relationship between displacement and tensile of PVDF nanofiber membrane, the maximum mechanical tensile strength is 0.97 MPa. Although the tensile is not large, the fluffy

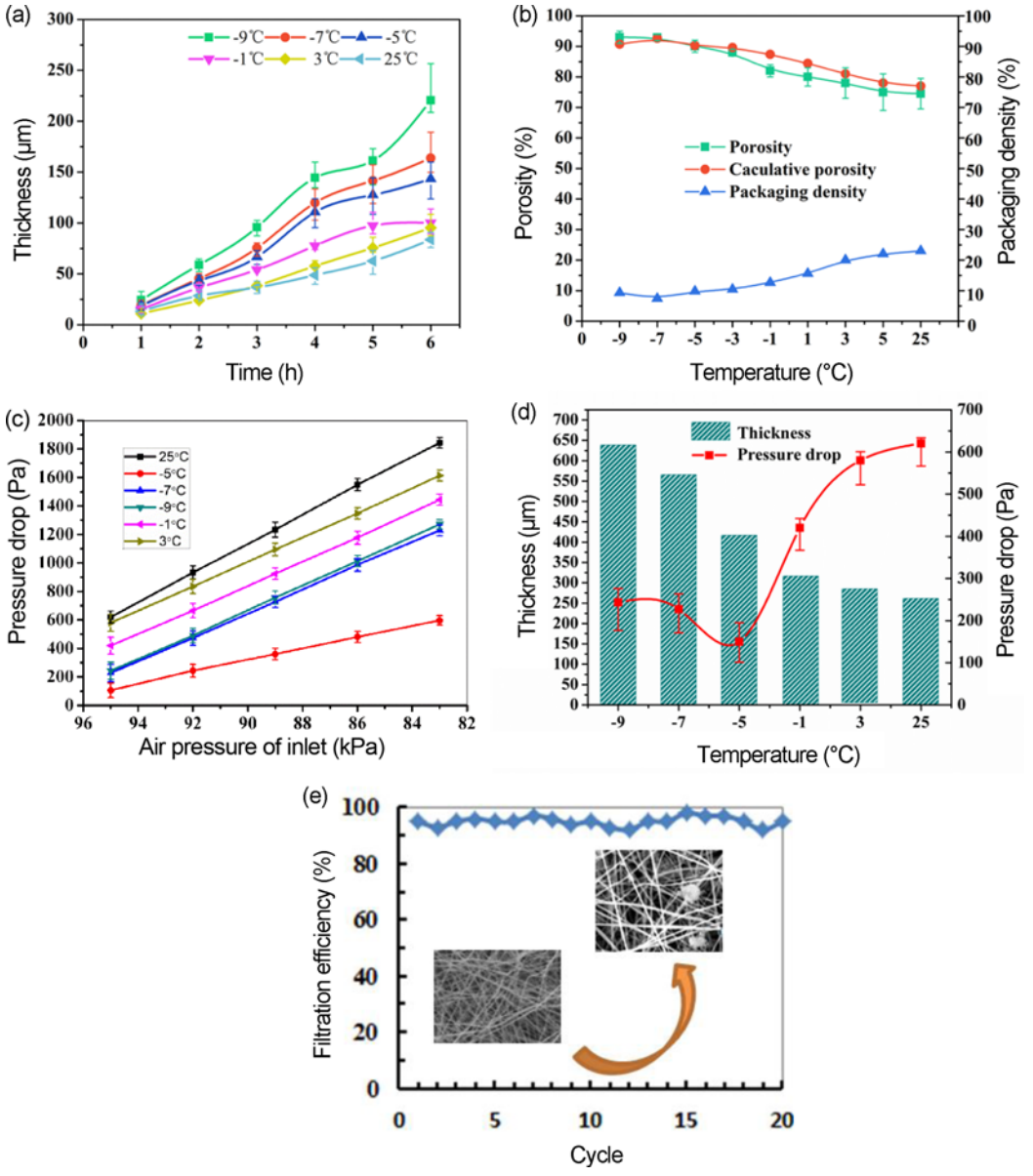

Figure 6. (a) The thickness of PVDF membranes under different temperature changes with electrospun time, (b) the porosity and packaging density of PVDF membranes under the various electrospinning temperatures, (c) the pressure drop of PVDF membranes changes with the air pressure of inlet, which have the same amount of time under different temperature, (d) the thickness and pressure drop of PVDF membranes based on the same time of electrospinning at different temperatures, and (e) removal efficiency of the membranes after multiple filtration cycles (-5 °C).

Table 2. Comprehensive performance of PVDF membranes

Temperature (°C)	Thickness (μm)	Porosity	Pressure drop (Pa)	Filtration time (s)
-7	83	0.901	123	14
-5	100.6	0.882	160	29
-1	97.4	0.81	420	52
3	95.2	0.78	580	79
25	90.6	0.773	620	84

structure is attached to basis material, and it barely withstands tension.

Filtration Performance of PVDF Membranes

Figure 8(a) is the the SEM image after filtered by the fiber membrane, and it can be found that many particles are blocked or adsorbed in the fiber membrane. Figure 8(b) shows the particles collected when the filter membrane is not used, and the particle size can be found between 100 nm

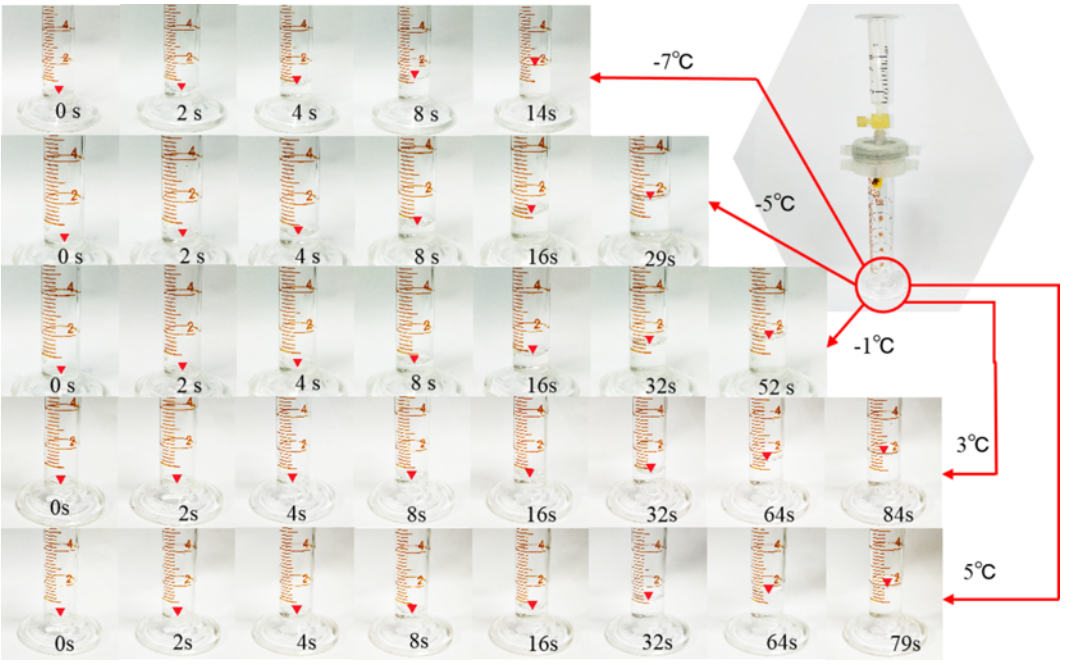

Figure 7. Liquid filtration process of PVDF electrospinning nanofiber membrane at different temperatures.

and 20 μm. Figure 8(c), (d) are the particles collected when the membranes are prepared by electrospinning at room temperature and low-temperature, respectively. It can be found that only a small amount of particles can be collected under the two processes, and the size is below 2 μm. This indicates that the PVDF nanofiber membrane has a better filtration effect and has the best filtering effect on particles over 2 μm. More importantly, the results show that the use of low-temperature electrospinning does not significantly reduce the filtration performance of PVDF nanofiber membranes.

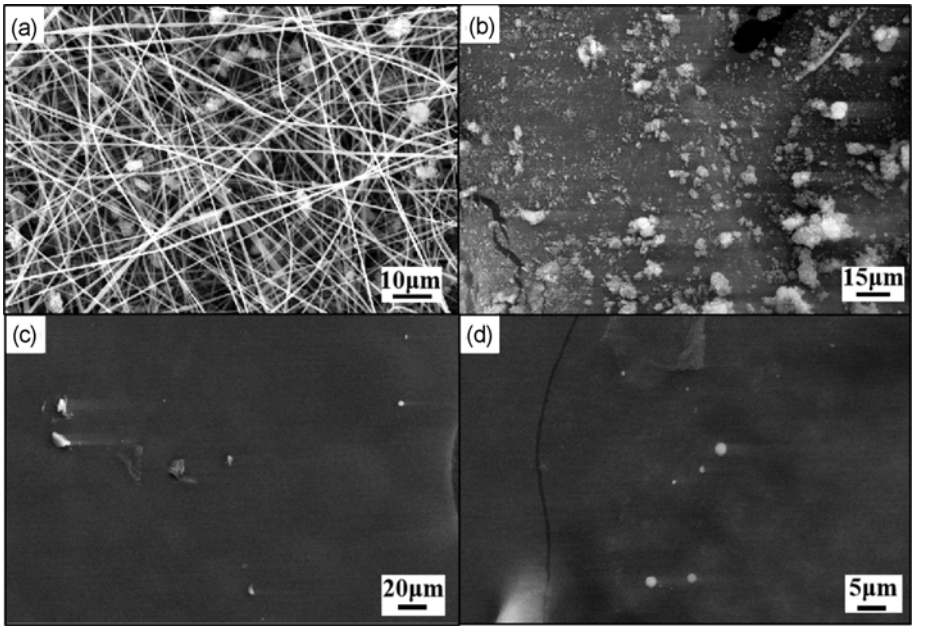

Figure 8. SEM images after filtered by the fiber membrane; (a) filtered PVDF fiber membranes, (b) particles collected without using filter membranes, (c), (d) particles collected when the membranes are prepared by electrospinning at room temperature and low-temperature, respectively.

Conclusion

Through the low-temperature electrospinning technology described in this paper, the nanofibrous membranes with high air permeability and fluffy structure can be obtained simply. And the two characteristics are more obvious with lower temperature. The speed of electrospun thickness at -9 °C is more than three times that of 25 °C, and the porosity can rise by 10-20 %. The pressure drop of PVDF nanofibrous membranes decrease to 123 Pa at the low-temperature, which is far lower than the room temperature (620 Pa). Meanwhile, the pore connectedness is better under low-temperature. The comprehensive performance achieves the best when the temperature remains at -5 °C due to the effect of thickness at the same electrospun time. At the same time, the filtration performance of the PVDF nanofiber membranes prepared by the low-temperature electrospinning does not reduce, and the filtration performance is still superior. The fascinating results provide a versatile strategy to fabricate nanofibrous membranes for various applications ranging from individual protection and industrial security to environmental governance.

Acknowledgements

This work was financially supported by Health and Education joint Tackling Plan of Fujian Province (No.WKJ2016-2-21) and The National Natural Science Foundation of China (No.61674125) and Aeronautical Science Funds (No.20160868004).

References

1. T. H. Kao, S. K. Su, C. I. Su, A. W. Lee, and J. K. Chen, *Aerosol. Sci. Tech*., **50**, 615 (2016).
2. K. Yoon, B. S. Hsiao, and B. Chu, *J. Mater. Chem*., **18**, 5326 (2008).
3. C. H. Hung and W. W. F. Leung, *Sep. Purif. Technol*., **79**, 34 (2011).
4. M. Zhu, J. Han, F. Wang, W. Shao, R. Xiong, Q. Zhang, H. Pan, Y. Yang, S. K. Samal, F. Zhang, and C. Huang, *Macromol. Mater. Eng*., **302**, 1600353 (2017).
5. E. Vijayakumar, A. Subramania, Z. Fei, and P. J. Dyson, *RSC Adv*., **5**, 52026 (2015).
6. M. Zhu, R. Xiong, and C. Huang, *Carbohydr. Polym*., **205**, 55 (2019).
7. M. Venkataraman, R. Mishra, J. Militky, X. Xiong, J. Marek, J. Yao, and G. Zhu, *Polym. Adavan. Technol*., **29**, 2583 (2018).
8. X. Mao, Y. Bai, J. Yu, and B. Ding, *J. Am. Ceram. Soc.,* **99**, 2760 (2016).
9. Q. Wang, F. Khan, L. Wei, H. Shen, and C. Zhang, *Sep. Purif. Technol*., **177**, 40 (2017).
10. W. Ma, Z. Guo, J. Zhao, Q. Yu, F. Wang, and J. Han, *Sep. Purif. Technol*., **177**, 71 (2017).
11. Y. Wang, W. Li, Y. Xia, X. Jiao, and D. Chen, *J. Mater. Chem. A,* **2**, 15124 (2014).
12. D. Lv, M. Zhu, Z. Jiang, S. Jiang, Q. Zhang, R. Xiong, and C. Huang, *Macromal. Mater. Eng*., **303**, 1800336 (2018).
13. D. Lv, R. Wang, G. Tang, Z. Mou, J. Lei, J. Han, S. D. Smedt, R. Xiong, and C. Huang, *ACS Appl. Mater. Interfaces*, **11**, 12880 (2019).
14. R. Wang, S. Guan, A. Sato, X. Wang, Z. Wang, and R. Yang, *J. Membrane Sci.,* **446**, 376 (2013).
15. X. Wang, Q. Fu, X. Wang, Y. Si, and J. Yu, *J. Mater. Chem. B*, **3**, 7281 (2015).
16. N. Wang, Y. Yang, S. S. Aldeyab, M. Elnewehy, J. Yu, and B. Ding, *J. Mater. Chem. A*, **3**, 23946 (2015).
17. X. Li, N. Wang, G. Fan, J. Yu, J. Gao, G. Sun, and B. Ding, *J. Colloid Interface Sci.,* **439**, 12 (2015).
18. J. P. Brincat, D. Sardella, A. Muscat, S. Decelis, J. N. Grima, and V. Valdramidis, *Trends Food Sci. Tech*., **50**, 175 (2016).
19. Y. S. Zhang, C. Y. Wang, L. Wang, J. W. Chen, and K. Qiao, *Adv. Mater. Res*., **726**, 2135 (2013).
20. W. W. F. Leung, C. H. Hung, and P. T. Yuen, *Sep. Purif. Technol.,* **71**, 30 (2010).
21. Q. P. Pham, U. Sharma, and A. G. Mikos, *Biomacromolecules,* **7**, 2796 (2006).
22. J. Wang, S. C. Kim, and D. Y. H. Pui, *J. Aerosol. Sci.,* **39**, 323 (2008).
23. S. Zhang, N. Tang, L. Cao, X. Yin, J. Yu, and B. Ding, *ACS Appl. Mater. Inter*., **8**, 29062 (2016).
24. M. Kucukali-Ozturk, E. Ozden-Yenigun, B. Nergis, and C. Candan, *J. Ind. Text*., **46**, 1498 (2017).
25. N. Vitchuli, Q. Shi, J. Nowak, M. Mccord, M. Bourham, and X. Zhang, *J. Appl. Polym. Sci*., **116**, 2181 (2010).
26. K. Liu, Z. Xiao, P. Ma, J. Chen, M. Li, Q. Liu, and D. Wang, *RSC Adv*., **5**, 87924 (2015).
27. H. Wan, N. Wang, J. Yang, Y. Si, K. Chen, and B. Ding, *J. Colloid Interf. Sci.,* **417**, 18 (2014).
28. X. Mao, Y. Si, Y. Chen, L. Yang, F. Zhao, and B. Ding, *RSC Adv*., **2**, 12216 (2012).
29. W. Li, Y. Xing, Y. Wu, J. Wang, L. Chen, and G. Yang, *Electrochim. Acta*, **151**, 289 (2015).
30. A. K. Selvam and G. Nallathambi, *Fiber. Polym*., **16**, 1327 (2015).
31. T. G. Kim, H. J. Chung, and T. G. Park, *Acta Biomater.,* **4**, 1611 (2008).
32. L. Bao, K. Seki, H. Niinuma, Y. Otani, R. Balgis, and T. Ogi, *Sep. Purif. Technol*., **159**, 100 (2016).
33. X. Wang, B. Ding, G. Sun, M. Wang, and J. Yu, *Prog. Mater. Sci*., **58**, 1173 (2013).
34. G. R. Xu, H. L. Zhao, and S. B. Wu, *Desalin. Water Treat*., **57**, 23522 (2016).
35. L. H. Lou, X. H. Qin, and H. Zhang, *Text. Res. J*., **87**, 208 (2017).
36. M. Simonet, O. D Schneider, P. Neuenschwander, and W. J. Stark, *Polym Eng Sci*., **47**, 2020 (2010).